

Impact Factor:

ISRA (India) = 4.971
ISI (Dubai, UAE) = 0.829
GIF (Australia) = 0.564
JIF = 1.500

SIS (USA) = 0.912
PIHHI (Russia) = 0.126
ESJI (KZ) = 8.716
SJIF (Morocco) = 5.667

ICV (Poland) = 6.630
PIF (India) = 1.940
IBI (India) = 4.260
OAJI (USA) = 0.350

SOI: [1.1/TAS](#) DOI: [10.15863/TAS](#)

International Scientific Journal Theoretical & Applied Science

p-ISSN: 2308-4944 (print) e-ISSN: 2409-0085 (online)

Year: 2019 Issue: 09 Volume: 77

Published: 24.09.2019 <http://T-Science.org>

QR – Issue



QR – Article



Denis Chemezov
Vladimir Industrial College,
M.Sc.Eng., Corresponding Member of International Academy of
Theoretical and Applied Sciences, Lecturer, Russian Federation
<https://orcid.org/0000-0002-2747-552X>
chemezov-da@yandex.ru

Alexandr Korobkov
Vladimir Industrial College,
Student, Russian Federation

Ilya Filippov
Vladimir Industrial College,
Student, Russian Federation

Evgeniy Varavin
Vladimir Industrial College,
Student, Russian Federation

Egor Salimov
Vladimir Industrial College,
Student, Russian Federation

Maxim Potapov
Vladimir Industrial College,
Student, Russian Federation

Elena Kiseleva
Vladimir Industrial College,
Master of Industrial Training, Russian Federation

INTERNAL FORCE FACTORS IN A SHEET BLANK MATERIAL WHEN DRAWING BY THE DIRECT METHOD

Abstract: Calculated dependencies of changing of internal force factors in a steel sheet blank from time of a drawing process by the direct method are presented in the article. The conclusion about influence of wrinkles formation on a flange of the sheet blank to changing of a value and a direction of forces and moments arising in material was given.

Key words: a sheet blank, drawing, force, moment, wrinkles, time.

Language: English

Citation: Chemezov, D., et al. (2019). Internal force factors in a sheet blank material when drawing by the direct method. *ISJ Theoretical & Applied Science*, 09 (77), 241-251.

Soi: <http://s-o-i.org/1.1/TAS-09-77-43> **Doi:**  <https://dx.doi.org/10.15863/TAS.2019.09.77.43>

Scopus ASCC: 2211.

Impact Factor:	ISRA (India) = 4.971	SIS (USA) = 0.912	ICV (Poland) = 6.630
	ISI (Dubai, UAE) = 0.829	PIHII (Russia) = 0.126	PIF (India) = 1.940
	GIF (Australia) = 0.564	ESJI (KZ) = 8.716	IBI (India) = 4.260
	JIF = 1.500	SJIF (Morocco) = 5.667	OAJI (USA) = 0.350

Introduction

Stamping of a sheet blank is characterized by various types of plastic deformation of material: bending, tension, compression and etc. Observation of the sheet blank drawing is difficult, because a deformation process is hidden by parts of a drawing die. Intensity of stress-strain state of the sheet blank material from all sides can be considered by a computer simulation. The various methods of shallow and deep drawing of the sheet blanks of round and square shapes made of various metal alloys in conditions of finite element modeling were considered in the works [1 – 19].

Wrinkles formation on a flange of the deformable round blank is due to excess material and a small thickness of a sheet. Deformation force of the blank increases in conditions of overcoming of material resistance by smoothing of wrinkles on side walls of the part in the die hole of the drawing die.

Action of external active forces (pressure and movement of a punch) leads to an emergence of internal force factors in material of the deformable sheet blank. These factors determine the value and the type of stresses (strains) in the sheet blank material. A calculated range of changes of the internal force factors will allow to select required force of drawing for performing of the process.

Materials and methods

The calculation of the internal force factors have been implemented in the LS-DYNA software environment. The round sheet blank model with the thickness of 2 mm had the volume of $2.5736 \times 10^{-5} \text{ m}^3$ and the surface area of 0.026532 m². The sheet blank drawing was performed by the direct method without a blank holder. Implementation conditions of the drawing process are presented in the special text format.

```
*TITLE
$   Created with ANSYS Workbench v14.5.7
$
$   Units: mm, mg, ms, mN, K
$

$$$$$$$$$$$$$$$$$$$$$$$$$$$$$$$$$$$$$$$$$$$$$$$$$$$$$$$$$$$$$$$$$$$$$$$$$$$$$$$$$$$$
$   SECTION DEFINITIONS                               $
$$$$$$$$$$$$$$$$$$$$$$$$$$$$$$$$$$$$$$$$$$$$$$$$$$$$$$$$$$$$$$$$$$$$$$$$$$$$$$$$$$$$
$
*SECTION_SOLID
$ 1SECID 2ELFORM 3AET
   1      1
*SECTION_SOLID
$ 1SECID 2ELFORM 3AET
   2      1
*SECTION_SOLID
$ 1SECID 2ELFORM 3AET
   3      1
$$$$$$$$$$$$$$$$$$$$$$$$$$$$$$$$$$$$$$$$$$$$$$$$$$$$$$$$$$$$$$$$$$$$$$$$$$$$$$$$$$$$
$   MATERIAL DEFINITIONS                              $
$$$$$$$$$$$$$$$$$$$$$$$$$$$$$$$$$$$$$$$$$$$$$$$$$$$$$$$$$$$$$$$$$$$$$$$$$$$$$$$$$$$$
$
*MAT_MODIFIED_PIECEWISE_LINEAR_PLASTICITY
$ 1MID 2RO 3E 4PR 5SIGY 6ETAN 7FAIL 8TDEL
$#  mid  ro  e  pr  sigy  etan  fail  tdel
   1 7.850000 2.0000E+8 0.300000 7.8500E+5 7.9300E+7
$  1C 2P 3LCSS 4LCSR 5VP 6EPSTHIN 7EPSMAJ 8NUMINT
$#   c  p  lcss  lcsr  vp  epsthin  epsmaj  numint
   0.000 0.000 0 0 0.000 0.000 0.000 0.000
$ 1EPS1 2EPS2 3EPS3 4EPS4 5EPS5 6EPS6 7EPS7 8EPS8
$#  eps1  eps2  eps3  eps4  eps5  eps6  eps7  eps8
   0.000 0.000 0.000 0.000 0.000 0.000 0.000 0.000
$ 1ES1 2ES2 3ES3 4ES4 5ES5 6ES6 7ES7 8ES8
$#  es1  es2  es3  es4  es5  es6  es7  es8
   0.000 0.000 0.000 0.000 0.000 0.000 0.000 0.000
*MAT_MODIFIED_PIECEWISE_LINEAR_PLASTICITY
$ 1MID 2RO 3E 4PR 5SIGY 6ETAN 7FAIL 8TDEL
$#  mid  ro  e  pr  sigy  etan  fail  tdel
```


Impact Factor:

ISRA (India)	= 4.971	SIS (USA)	= 0.912	ICV (Poland)	= 6.630
ISI (Dubai, UAE)	= 0.829	PIHI (Russia)	= 0.126	PIF (India)	= 1.940
GIF (Australia)	= 0.564	ESJI (KZ)	= 8.716	IBI (India)	= 4.260
JIF	= 1.500	SJIF (Morocco)	= 5.667	OAJI (USA)	= 0.350

```

*BOUNDARY_PRESCRIBED_MOTION_SET_ID
$ 1KeyID 2HEADING
  1Displacement 2
$ 1ID 2DOF 3VAD 4LCID 5SF 6VID 7DEATH 8BIRTH
  4 1 2 5 1.000 0 0 0
*BOUNDARY_PRESCRIBED_MOTION_SET_ID
$ 1KeyID 2HEADING
  2Displacement 2
$ 1ID 2DOF 3VAD 4LCID 5SF 6VID 7DEATH 8BIRTH
  4 2 2 6 1.000 0 0 0
*BOUNDARY_PRESCRIBED_MOTION_SET_ID
$ 1KeyID 2HEADING
  3Displacement 2
$ 1ID 2DOF 3VAD 4LCID 5SF 6VID 7DEATH 8BIRTH
  4 3 2 7 1.000 0 0 0
*BOUNDARY_SPC_SET
$ 1NSID 2CID 3DOFX 4DOFY 5DOFZ 6DOFRX 7DOFRY 8DOFRZ
  1 0 1 1 1 1 1 1

```

where **1**, **2** and **3** – the models identifiers of the punch, the sheet blank and the die; ***TITLE** – heading to appear on output and in output files; ***SECTION_SOLID** – the section properties for solid continuum and fluid elements; **1SECID** – the section ID; **2ELFORM** – the element formulation options; **3AET** – the ambient element type; ***MAT_MODIFIED_PIECEWISE_LINEAR_PLASTICITY** – elasto-plastic material supporting the arbitrary stress versus strain curve as well as the arbitrary strain rate dependency; **1MID** – the material identification; **2RO** – mass density; **3E** – the Young's modulus; **4PR** – the Poisson's ratio; **5SIGY** – yield stress; **6ETAN** – the tangent modulus; **7FAIL** – the failure flag; **8TDEL** – the minimum time step size for the automatic element deletion; **1C**, **2P** – the strain rate parameters; **3LCSS** – the load curve ID or the table ID; **4LCSR** – the load curve ID defining strain rate scaling effect on yield stress; **5VP** – the formulation for rate effects; **6EPSTHIN** – thinning strain at failure; **7EPSMAJ** – major in plane strain at failure; **8NUMINT** – the number of the integration points which must fail before the element is deleted; **1EPS1** – **8EPS8** – the effective plastic strain values; **1ES1** – **8ES8** – the yield stress values; ***MAT_PLASTIC_KINEMATIC** – the model of isotropic and kinematic hardening plasticity with the option of including rate effects; **7BETA** – the hardening parameter; **src** – the strain rate parameter, *C*, for the Cowper Symonds strain rate model; **srp** – the strain rate parameter, *P*, for the Cowper Symonds strain rate model; **fs** – effective plastic strain for the eroding elements; **vp** – the formulation for rate effects; ***PART** – the define parts, i.e., the combine material information, the section properties, the hourglass type, the thermal properties, and the flag for the part adaptivity; **HEADING** – heading for the part; **1PID** – the part identification; **2SECID** – the section identification; **3MID** – the material identification; **4EOSID** – the equation of the state identification;

5HGID – the hourglass/bulk viscosity identification; **6GRAV** – the flag to turn on gravity initialization; **7ADPORT** – indicate if this part is adapted or not; **8TMID** – the thermal material property identification; ***DEFINE_CURVE** – define the curve, for example, load versus time, often loosely referred to as the load curve; **1LCID** – the load curve ID; **2SIDR** – the flag controlling use of the curve during dynamic relaxation; **3SFA** – the scale factor for the abscissa value; **4SFO** – the scale factor for the ordinate value; **5OFFA** – offset for the abscissa values; **6OFFO** – offset for the ordinate values; **7DATTYP** – the data type; **1A** – the abscissa values; **2O** – the ordinate values; ***CONTACT_AUTOMATIC_SINGLE_SURFACE** – the contact interface in the 3D model; **1SSID** – the slave segment, the node set ID, the part set ID, the part ID, or the shell element set ID; **2MSID** – the master segment set ID, the part set ID, the part ID, or the shell element set ID; **3SSTYP** – the ID type of SSID; **4MSTYP** – the ID type of MSID; **5SBOXID** – include in contact definition only those slave nodes/segments within box; **6MBOXID** – include in contact definition only those master segments within box; **7SPR** – the slave side forces included; **8MPR** – the master side forces included; **1FS** – the static coefficient of friction; **2FD** – the dynamic coefficient of friction; **3DC** – the exponential decay coefficient; **4VC** – the coefficient for viscous friction; **5VDC** – the viscous damping coefficient in percent of critical or the coefficient of restitution expressed as percentage; **6PENCHK** – small penetration in the contact search option; **7BT** – birth time (the contact surface becomes active at this time); **8DT** – death time (the contact surface is deactivated at this time); **1SFS** – the scale factor on default slave penalty stiffness; **2SFM** – the scale factor on default master penalty stiffness; **3SST** – the optional contact thickness for the slave surface; **4MST** – the optional contact thickness for the master surface; **5SFST** – the scale factor applied to the

Impact Factor:

ISRA (India)	= 4.971	SIS (USA)	= 0.912	ICV (Poland)	= 6.630
ISI (Dubai, UAE)	= 0.829	PIHHI (Russia)	= 0.126	PIF (India)	= 1.940
GIF (Australia)	= 0.564	ESJI (KZ)	= 8.716	IBI (India)	= 4.260
JIF	= 1.500	SJIF (Morocco)	= 5.667	OAJI (USA)	= 0.350

contact thickness of the slave surface; **6SFMT** – the scale factor applied to the contact thickness of the master surface; **7FSF** – the Coulomb friction scale factor; **8VSF** – the viscous friction scale factor; **1SOFT** – the soft constraint option; **2SOFSC** – the scale factor for constraint forces of the soft constraint option; **3LCIDAB** – the load curve ID defining the airbag thickness as the function of time; **4MAXPAR** – the maximum parametric coordinate in the segment search; **5SBOPT** – the segment-based contact options; **6DEPTH** – the search depth in automatic contact; **7BSORT** – the number of cycles between bucket sorts; **8FRCFRQ** – the number of cycles between contact force updates for the penalty contact formulations; ***CONTROL_TERMINATION** – stop the job; **1ENDTIM** – termination time; **2ENDCYC** – termination cycle; **3DTMIN** – the reduction factor to determine the minimum time step; **4ENDENG** – percent change in the energy ratio for termination of the calculation; **5ENDMAS** – percent change in the total mass for termination of the calculation; ***CONTROL_TIMESTEP** – the set structural time step size control using the different options; **1DTINIT** – the initial time step size; **2TSSFAC** – the scale factor for the computed time step; **3ISDO** – basis of the time size calculation for 4-node shell elements; **4TSLIMIT** – the shell element minimum time step assignment; **5DT2MS** – the time step size for the mass scaled solutions; **6LCTM** – the load curve ID that limits the maximum time step size (optional); **7ERODE** – the erosion flag for the solids and thick shells; **8MS1ST** – the option for the mass scaling; ***CONTROL_HOURLASS** – redefine the default values of the hourglass control type and the coefficient; **1IHQ** – the default hourglass control type; **2QH** – the default hourglass coefficient; ***CONTROL_BULK_VISCOSITY** – reset the default values of the bulk viscosity coefficients globally; **1Q1** – the default quadratic viscosity coefficient; **2Q2** – the default linear viscosity coefficient; **3TYPE** – the default bulk viscosity type; ***CONTROL_CONTACT** – change defaults for computation with the contact surfaces; **1SLSFAC** – the scale factor for the sliding interface penalties; **2RWPAL** – the scale factor for the rigid wall penalties, which the treat nodal points interacting with the rigid walls; **3ISLCHK** – initial penetration check in the contact surfaces with indication of initial penetration in the output files; **4SHLTHK** – the flag for consideration of the shell thickness offsets in the non-automatic surface-to-surface and non-automatic nodes-to-surface type contacts; **5PENOPT** – the penalty stiffness value option; **6THKCHG** – the shell thickness changes considered in the single surface contact; **7ORIEN** – optional automatic reorientation of the contact interface segments during initialization; **8ENMASS** – treatment of the mass of the eroded nodes in contact; **1USRSTRC** – storage per the contact interface for the user supplied interface control

subroutine; **2USRFRFC** – storage per the contact interface for the user supplied interface friction subroutine; **3NSBCS** – the number of cycles between contact searching using three dimensional bucket searches; **4INTERM** – the flag for intermittent searching in the old surface-to-surface contact using the interval; **5XPENE** – the contact surface maximum penetration check multiplier; **6SSTHK** – the flag for using the actual shell thickness in the single surface contact; **7ECDT** – the time step size override for eroding contact; **8TIEDPRJ** – bypass projection of the slave nodes to the master surface in the types; **1SFRIC** – the default static coefficient of friction; **2DFRIC** – the default dynamic coefficient of friction; **3EDC** – the default exponential decay coefficient; **4VFC** – the default viscous friction coefficient; **5TH** – the default contact thickness; **6TH_SF** – the default thickness scale factor; **7PEN_SF** – the default local penalty scale factor; **1IGNORE** – ignore initial penetrations; **2FRCENG** – the flag to activate the calculation of frictional sliding energy; **3SKIPRWG** – the flag not to display the stationary rigid wall by default; **4OUTSEG** – the flag to output each beam spot weld slave node and its master segment; **5SPOTSTP** – the spot weld node or the face; **6SPOTDEL** – this option controls the behavior of spotwelds when the parent element erodes; **7SPOTTHIN** – the optional thickness scale factor; ***CONTROL_SOLID** – provide controls for the solid element response; **1ESORT** – automatic sorting of the tetrahedral and pentahedral elements to avoid use of the degenerate formulations for these shapes; **2FMATRX** – the default method used in the calculation of the deformation gradient matrix; **3NIPTETS** – the number of the integration points used in the quadratic tetrahedron elements; **4SWLOCL** – the output option for stresses in the solid elements used as spot welds; ***DAMPING_GLOBAL** – define the mass weighted nodal damping that applies globally to the nodes of deformable bodies and to the mass center of the rigid bodies; **1LCID** – the load curve ID which specifies the system damping constant vs. time; **2VALDMP** – the system damping constant, *D_s*; **3STX** – the scale factor on the global X translational damping forces; **4STY** – the scale factor on the global Y translational damping forces; **5STZ** – the scale factor on the global Z translational damping forces; **6SRX** – the scale factor on the global X rotational damping moments; **7SRY** – the scale factor on the global Y rotational damping moments; **8SRZ** – the scale factor on the global Z rotational damping moments; ***CONTROL_ENERGY** – provide controls for the energy dissipation options; **1HGEN** – the hourglass energy calculation option; **2RWEN** – the rigidwall energy (a.k.a. stonewall energy) dissipation option; **3SLNTEN** – the sliding interface energy dissipation option; **4RYLEN** – the Rayleigh energy dissipation option; ***CONTROL_ACCURACY** – the define

Impact Factor:	ISRA (India) = 4.971	SIS (USA) = 0.912	ICV (Poland) = 6.630
	ISI (Dubai, UAE) = 0.829	PPIIH (Russia) = 0.126	PIF (India) = 1.940
	GIF (Australia) = 0.564	ESJI (KZ) = 8.716	IBI (India) = 4.260
	JIF = 1.500	SJIF (Morocco) = 5.667	OAJI (USA) = 0.350

control parameters that can improve the accuracy of the calculation; **1OSU** – the global flag for the 2nd order objective stress updates; **2INN** – the invariant node numbering for the shell and solid elements; **3PIDOSU** – the part set ID for objective stress updates; ***DATABASE_GLSTAT** – the global data; **1DT** – the time interval between outputs; **2BINARY** – the flag for binary output; **3LCUR** – the optional curve ID specifying the time interval between dumps; **4IOOPT** – the flag to govern behavior of the plot frequency load curve; **5DTHFF**, **6BINHF** – no data; ***DATABASE_MATSUM** – material energies; ***DATABASE_NODOUT** – the nodal point data; ***DATABASE_ELOUT** – the element data; ***DATABASE_BINARY_D3PLOT** – the database for the entire model; **2LCDT** – the optional load curve ID specifying the time interval between dumps; **3BEAM** – the discrete element option flag; **4NPLTC** – this overrides the DT specified in the first field; ***DATABASE_BINARY_RUNRSF** – the database for restarts; **2NR** – the number of the RUNning ReStart Files, runrsf, written in the cyclical fashion; ***LOAD_NODE_SET** – apply concentrated nodal force to the node or each node in the set of the nodes; **1ID** – the node ID or the nodal set ID; **2DOF** – applicable degrees-of-freedom; **3LCID** – the load curve ID; **4SF** – the load curve scale factor; **5CID** – the coordinate system ID; **6M1** – the node 1 ID; **7M2**

– the node 2 ID; **8M3** – the node 3 ID; ***BOUNDARY_PRESCRIBED_MOTION_SET_ID** – define the imposed nodal motion (velocity, acceleration or displacement) on the node or the set of the nodes; **3VAD** – the velocity/acceleration/displacement flag; **6VID** – the vector ID; **7DEATH** – time the imposed motion/constraint is removed; **8BIRTH** – time that the imposed motion/constraint is activated; ***BOUNDARY_SPC_SET** – the option is required since it specifies whether the SPC applies to the single node or to the set; **3DOFX** – the insert 1 for the translational constraint in the local X-direction; **4DOFY** – the insert 1 for the translational constraint in the local Y-direction; **5DOFZ** – the insert 1 for the translational constraint in the local Z-direction; **6DOFRX** – the insert 1 for the rotational constraint about the local X-axis; **7DOFRY** – the insert 1 for the rotational constraint about the local Y-axis; **8DOFRZ** – the insert 1 for the rotational constraint about the local Z-axis.

Results and discussion

The calculated dependencies of changing of the internal force factors when drawing of the round steel sheet blank with the thickness of 2 mm from performing time of the plastic deformation process are presented in the Fig. 1.

Impact Factor:

ISRA (India) = 4.971	SIS (USA) = 0.912	ICV (Poland) = 6.630
ISI (Dubai, UAE) = 0.829	PIHHI (Russia) = 0.126	PIF (India) = 1.940
GIF (Australia) = 0.564	ESJI (KZ) = 8.716	IBI (India) = 4.260
JIF = 1.500	SJIF (Morocco) = 5.667	OAJI (USA) = 0.350

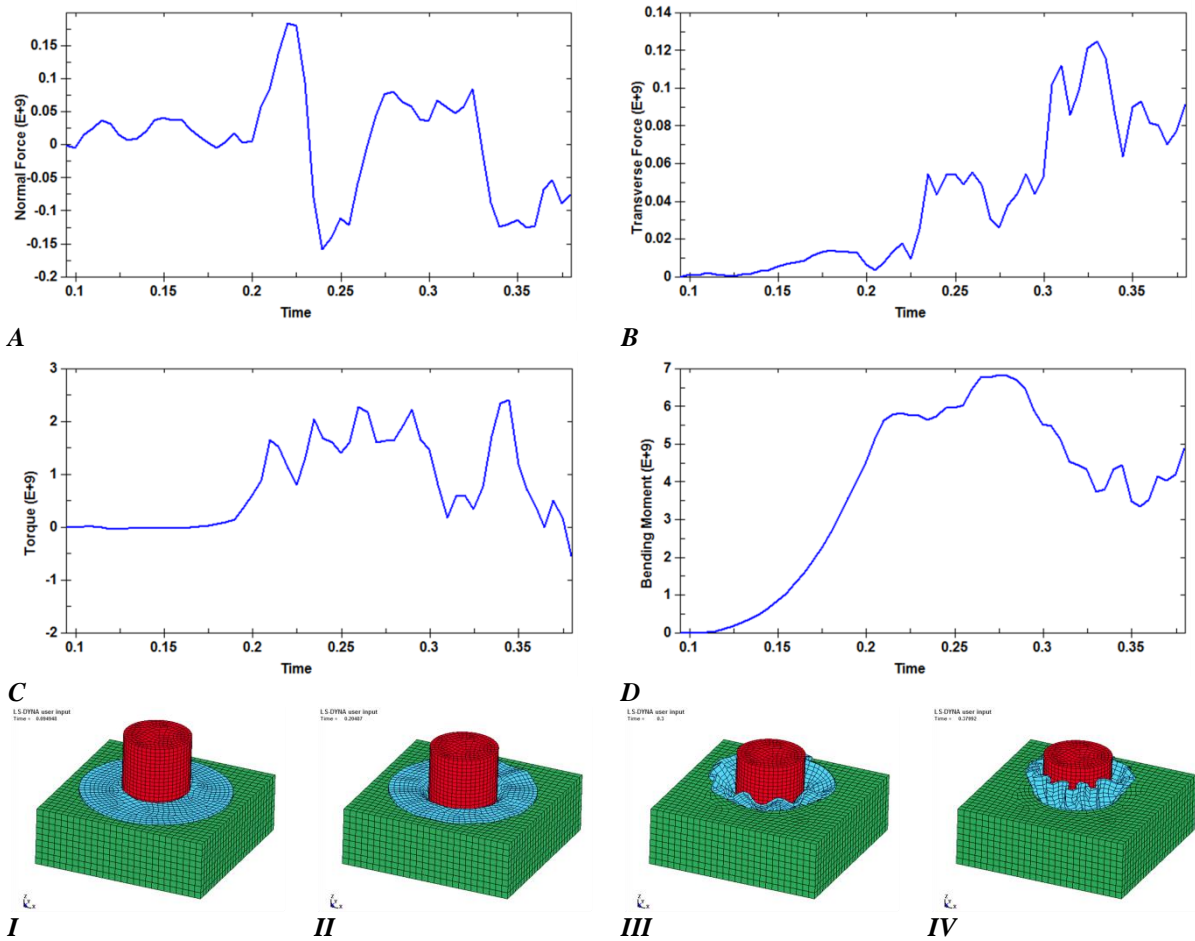


Figure 1 – The internal force factors in material of the sheet blank when drawing: A – changing of normal force from time drawing; B – changing of transverse force from time drawing; C – changing of torque from time drawing; D – changing of bending moment from time drawing; I – deformation of the sheet blank at 0.095 s of the drawing process; II – deformation of the sheet blank at 0.2 s of the drawing process; III – deformation of the sheet blank at 0.3 s of the drawing process; IV – deformation of the sheet blank at 0.38 s of the drawing process.

The drawing process of the sheet blank was depicted in the three-dimensional statement: 0.095 s – the end surface of the punch touches the flange of the sheet blank; 0.2 s – beginning of wrinkles formation on the flange; 0.3 s – increasing of wrinkles radii on the flange; 0.38 s – finishing of the drawing process. The values of normal force characterize a deformation degree of compression and tension of the sheet blank material. The sheet blank is subjected to alternating deformations of tension and compression over the entire time range of the drawing process. The maximum values of compression and tension of material are observed on the small time range of the deformation process at the stage of active formation of wrinkles. Gradual punching of the sheet blank into the die hole leads to increasing of transverse force by 6 times. Changes of transverse force are associated with the smoothing process of wrinkles on the sheet

blank in the die hole. Transverse force is less than normal force. The calculation results show that torque acts clockwise and counterclockwise in the blank material. The negative values of torque were determined only in the end of the drawing process. Bending moment acts only in one direction when drawing. The maximum value of bending moment reaches at the stage of active formation of wrinkles. Bending moment is more than torque.

The dependence of changing of the deformation area of the steel sheet blank from time of the drawing process is presented in the Fig. 2.

The deformation area of the sheet blank in beginning of the drawing process is equal to the area of the end surface of the punch. The deformation area increases by 20% of the initial area of material deformation at the stage of wrinkles formation.

Impact Factor:

ISRA (India)	= 4.971	SIS (USA)	= 0.912	ICV (Poland)	= 6.630
ISI (Dubai, UAE)	= 0.829	PPIHJ (Russia)	= 0.126	PIF (India)	= 1.940
GIF (Australia)	= 0.564	ESJI (KZ)	= 8.716	IBI (India)	= 4.260
JIF	= 1.500	SJIF (Morocco)	= 5.667	OAJI (USA)	= 0.350

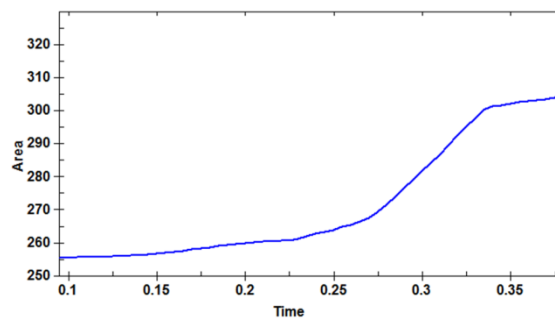


Figure 2 – Changing of the deformation area of the sheet blank from time of the drawing process.

Conclusion

In the direction of the axial line of the round sheet blank there is more plastic deformation of material than in the transverse direction. The drawing process occurs intermittently due to uneven of distribution and the different sizes of wrinkles on the

sheet blank. Rational force of drawing of the round steel sheet blanks of the small thickness without using of the blank holder can be determined by the calculated maximum values of the internal force factors.

References:

1. Chemezov, D. A., Seliverstov, V. S., & Kondrakov, A. A. (2015). The process of corrugations formation on a flange of deformable sheet material. *Scientific and practical journal "Journal of scientific and applied researches"*, №10, 79-81.
2. Chemezov, D. A. (2015). The research of the shallow drawing process of the plate stock. *ISJ Theoretical & Applied Science*, 10 (30), 11-15.
3. Chemezov, D. A., Seliverstov, V. S., Komisar, A. S., Zezina, N. A., & Tyurina, S. I. (2015). Stamping of the plate stock with blank holder: the character of the material deformation and calculation of the coefficient of elongation. *ISJ Theoretical & Applied Science*, 11 (31), 101-107.
4. Chemezov, D. A. (2015). Changing the wall thickness of the hollow detail during a shallow drawing of the plate stock. *ISJ Theoretical & Applied Science*, 12 (32), 34-37.
5. Chemezov, D. A., Seliverstov, V. S., Bayakina, A. V., & Zezina, N. A. (2016). The influence of the magnitude of the radius chamfer in the die hole on the degree of deformation of the processed material and the productivity of the deep drawing process of the plate stock. *ISJ Theoretical & Applied Science*, 01 (33), 52-57.
6. Chemezov, D. A., Smirnova, L. V., Seliverstov, V. S., & Zezina, N. A. (2016). Comparison of stress-strain state of thin-walled detail after deep drawing of the direct and reverse methods. *ISJ Theoretical & Applied Science*, 03 (35), 21-25.
7. Chemezov, D. A. (2016). The drawing of the plate stock without blank holder. *ISJ Theoretical & Applied Science*, 07 (39), 1-6.
8. Chemezov, D. A., & Seliverstov, V. S. (2015). The intensity of the formation of corrugation on the flange of the deformable plate stock of thickness 1-5 mm. *Scientific and theoretical journal "System engineering"*, №2, 71-76.
9. Chemezov, D. A. (2016). The calculation of the maximum stress of thin-walled detail while performing the technological process of deep drawing of the plate stock. *Fundamental and applied researches in the modern world. Materials of the XIII International scientific and practical conference, Volume 1*, 36-39.
10. Chemezov, D. A., Seliverstov, V. S., & Zezina, N. A. (2016). Analysis of the technological process of deep drawing of a thin-walled part: processing modes, sizes of forming tools and rejects. *International scientific journal "Young scientist"*, №4, 101-105.
11. Chemezov, D. A., Zezina, N. A., & Seliverstov, V. S. (2015). The determination of the bending moment at the pressure of the punch on the material in the conditions of the shallow drawing of the plate stock. *Fundamental and applied researches in the modern world. Materials of the*

Impact Factor:

ISRA (India) = 3.117
ISI (Dubai, UAE) = 0.829
GIF (Australia) = 0.564
JIF = 1.500

SIS (USA) = 0.912
PIHHI (Russia) = 0.126
ESJI (KZ) = 8.716
SJIF (Morocco) = 5.667

ICV (Poland) = 6.630
PIF (India) = 1.940
IBI (India) = 4.260
OAJI (USA) = 0.350

- XII International scientific and practical conference, Volume 1, 73-76.*
12. Galkin, V. V., Pozdyshev, V. A., Vashurin, A. V., & Pachurin, G. V. (2013). Mathematical modeling of the production of an article type by deep hot glass dome on the basis of software, Deform. *Fundamental Research, №1*, 371-374.
 13. Zolotov, M. A., Galkin, V. V., & Schevchenko, M. P. (1990). Hood parts with differential heating of billets in the radial direction. *Forging and stamping production, no. 7*, 14-16.
 14. Tóth, L. S., Hirsch, J., & Houtte, P. (1996). On the role of texture development in the forming limits of sheet metals. *International Journal of Mechanical Sciences, vol. 38, issue 10*, 1117-1126.
 15. Shlyapugin, A. G., & Tsytsorin, D. A. (2013). Investigation process hoods slide in conical matrix using DEFORM-2D. *Academic Journal "Izvestia of Samara Scientific Center of the Russian Academy of Sciences", vol. 15, №6*, 262-266.
 16. Chemezov, D., et al. (2019). Manufacturing of a case-shaped part in conditions of sheet stamping. *ISJ Theoretical & Applied Science, 05 (73)*, 51-64.
 17. Chemezov, D. A., Smirnova, L. V., & Seliverstov, V. S. (2016). The calculation of the sizes of the plate stock for the processing of thin-walled details of the square shape by the method of deep drawing. *ISJ Theoretical & Applied Science, 04 (36)*, 111-114.
 18. Chemezov, D., & Lukyanova, T. (2017). A determination of the strain state of the thin-walled hollow detail of square shape after the drawing of the sheet metal with the blank holder. *ISJ Theoretical & Applied Science, 01 (45)*, 64-66.
 19. Chemezov, D. A. (2019). Modeling of a technological process of a square part drawing. *Electronic scientific journal of the Vladimir industrial college, №1*, 4-6.